

## EVALUATION OF THE BIOLOGICAL EFFECT SYNTHESIZED ZINC OXIDE NANOPARTICLES ON *PSEUDOMONAS AERUGINOSA*

\*M. A. Alaa Alden  
Researcher

\*L. A. Yaaqoob  
Assnt.prof.

\*Department of Biotechnology, Science College, University of Baghdad, Baghdad, Iraq  
Maram.1995.a95@gmail laith.yaaqoob@sc.uobaghdad.edu.iq

### ABSTRACT

This study was aimed to demonstrate the biosynthesis procedure of Zinc oxide nanoparticles (ZnO NPs) using Prodigiosin pigment which in turn produced from particular environmental bacteria isolates *Serratiamarcescens* a stabilizing and reducing agent. Additionally, the synthesis conditions were precisely taken into consideration as a pH of 7 and a temperature of 50°C alongside a concentration of prodigiosin of 12 mg/ml with 5mg precursor of zinc acetate in deionized distilled water (DDW) 50ml. Biosynthesized ZnO nanoparticles have presented many applications such as catalysis, biosensing, anticancer, and biomedical, etc. The optimum condition for ZnO biosynthesis was characterized through several techniques such as UV-Vis, AFM, XRD, FT-IR, and FE-SEM. In particular, a cut-off phenomenon of the biological synthesized ZnO was found at around 280 nm using UV-Vis, while spherical shape particles were noticed using FE-SEM techniques. Also, the AFM analysis revealed that ZnO NPs an average diameter size of 45.02 nm. And the effect of ZnO NPs on bacteria *Pseudomonas aeruginosa* on an inhibition zone 29mm.

Keywords: ZnO nanoparticles, antimicrobial activity, prodigiosin.

علاء و يعقوب

مجلة العلوم الزراعية العراقية -2022: 53(1): 27-37

تقييم التأثير البيولوجي لجسيمات اوكسيد الزنك المصنعة النانوية على بكتريا *pseudomonas aeruginosa*

ليث احمد يعقوب  
استاذ مساعد

مرام احمد علاء  
باحث

قسم التقنيات الأحيائية، كلية العلوم، جامعة بغداد، بغداد، العراق.

المستخلص :

هدفت هذه الدراسة الى توضيح إجراء التخليق الحيوي لجسيمات اوكسيد الزنك النانوية (ZnO NPs) باستخدام صبغة Prodigiosin التي تنتج بدورها من بكتيريا بيئية معينة *Serratia marcescens* كعامل استقرار واختزال. بالإضافة إلى ذلك، تم أخذ ظروف التوليف في الاعتبار بدقة على أنها درجة حموضة 7 ودرجة حرارة 50 درجة مئوية جنباً الى جنب مع تركيز بروديجوسين 12 مجم / ملمع 5 ملمع من خلاصات الزنك في الماء المقطر منزوع الأيونات (DDW) 50 مل. قدمت جسيمات ZnO النانوية المصنعة حيوياً العديد من التطبيقات مثلًا لتحفيز، والاستشعار الحيوي، ومضاد السرطان، والطب الحيوي، وما إلى ذلك. تميزت الحالة المثلى لتخليق ZnO NPs الحيوي من خلال العديد من التقنيات مثل UV-Vis و AFM و XRD و FT-IR على وجه الخصوص، تم العثور على ظاهرة الانقطاع لـ ZnO للمركب البيولوجي عند حوالي 280 نانومتر باستخدام تقنيات UV-Vis، بينما لوحظت جزيئات الشكل الكروية باستخدام FE-SEM. وكذلك، كشف فحص AFM أن معدل حجم الجسيمات ZnO NPs يبلغ 45.02 نانومتر. وإن تأثير الزنك النانوي على بكتريا *Pseudomonas aeruginosa* بتثبيط نمو بكتيري هو 29 ملم.

الكلمات المفتاحية: جزيئات أكسيد الزنك النانوية، نشاط مضاد للميكروبات، بروديجوسين.

## INTRODUCTION

*Pseudomonas aeruginosa* is a widely known Gram-negative bacterium that is isolated using several clinical sources. This type of bacterium is characterized using the Vitek-2 system, polymerase chain reaction (PCR), and biochemical tests. Specifically, the antibiotic susceptibility revealed that *P. aeruginosa* possesses some resistance to Methicillin and Nitrofurantoin as well as a noticeable sensitivity to colistin and Ciprofloxacin. Among Gram-negative bacteria *Pseudomonas aeruginosa* is a rod-shaped, motile bacterium that is capable of growing in both anaerobic and aerobic manners. Gram-negative bacteria are known as a major cause of nosocomial infections, leading to an extended period of hospitalization, mortality rate, and higher hospitalization charges (1). The *P. aeruginosa* can be located in several moist environments and able to grow in many others. This particular adaptable pathogen is frequently linked to clinical infections, specifically in immunocompromised patients. Furthermore, this type of bacteria is worldwide considered as one of the most commonly recovered pathogens within the intensive care unit (ICU) patients. Moreover, wide-ranging reports of nosocomial infection due to this particular bacterium are common, typically caused by the hospital environment and cross-contamination which is related to the improper utilization of medical devices/equipment (2, 3, 4, 5). Additionally, the majority of infections that occur in immunodeficiency patients result from mucous membrane loss. The latter is attributed to the germination mechanism existence which in turn is caused by antibiotic resistance (6). Antibiotic is a natural substance that inhibits many microbes' activity, such as bacteriostatic (7, 8). Nanoparticles and nanobiomedicine provide an alternative pathway to overcoming the addressed typical antibiotic limitations due to excellent biocompatibility, high antimicrobial activity, and good thermal

stability of the nanoparticles (9, 10). Several nanoparticles, ZnO in particular, delivers an outstanding antimicrobial performance in a wide range of bacteria such as *Escherichia coli* and *Staphylococcus aureus* (9, 11). Furthermore, ZnO has demonstrated some attractive applications such as solar cells, catalysts, photodetectors, and biomedical/antibacterial activity (12, 13, 14, 15). Herein, the interaction between the bacteria and ZnO nanoparticles are highly effective if the ZnO is prepared using a biological method due to the absence of undesired/toxic chemical compounds. Also, ZnO nanoparticles are biocompatible and non-toxic (16, 17, 18). The aforementioned advantages provide great potential in the utilization of ZnO nanoparticles as an antibacterial agent. Therefore, this study aims to evaluate the antibacterial activity of ZnO nanoparticles against Gram-negative *P. aeruginosa* through a biosynthesis approach using Prodigiosin as a reducing agent.

## MATERIALS AND METHODS

**Bacterial isolation and culture media:** In this study, the isolated bacteria (*p. aeruginosa*) were collected from December 2019 to February 2020 from three different hospitals namely, Sheikh Zayed, Al-Yarmouk, and Baghdad/Medical city; this includes 210 clinical specimens' comparison concerning urine and wounds. The collected specimens were directly streaked on macconkey agar and subsequently incubated at 37 °C for 24 hr. Using macconkey agar, the corresponded specimens were found to be black colonies, while another test such as the biological and morphological analysis was also performed (19, 20). Furthermore, identification of the collected specimens was demonstrated via automated and/or manual techniques (Vitek II, bioMérieux, Marcy l'Etoile, France); the attained Vitek II outcomes are presented in Figure 1.

bioMérieux Customer:	Microbiology Chart Report	Printed Sep 3, 2020 21:58 CDT
Patient Name:		Patient ID:
Location:		Physician:
Lab ID: 03		Isolate Number: 1
Organism Quantity:		
Selected Organism : <i>Pseudomonas aeruginosa</i>		

Source: \_\_\_\_\_ Collected: \_\_\_\_\_

Comments:	

Susceptibility Information			Analysis Time: 15.58 hours			Status: Final		
Antimicrobial	MIC	Interpretation	Antimicrobial	MIC	Interpretation			
Ticarcillin	>= 128	R	Amikacin	<= 2	S			
Ticarcillin/Clavulanic Acid	>= 128	R	Gentamicin	<= 1	S			
Piperacillin	16	*R	Tobramycin	<= 1	S			
Piperacillin/Tazobactam	32	S	Ciprofloxacin	<= 0.25	S			
Ceftazidime	4	S	+Levofloxacin		S			
+Ceftriaxone		R	Pefloxacin					
Cefepime	2	S	Minocycline					
Aztreonam			Colistin	<= 0.5	S			
Imipenem	2	S	Rifampicin					
Meropenem	2	S	Trimethoprim/Sulfamethoxazole					

+= Deduced drug \*= AES modified \*\*= User modified

AES Findings	
Confidence:	Consistent

**Figure 1. Vitek II test for *Pseudomonas aeruginosa*s**

**Prodigiosin pigment production:** In a typical procedure, the fermentation media was prepared by (21). In detail, the corresponded media was attained by mixing peptone (5g/L) and source sucrose (10g/L) as the nitrogen and carbon sources, respectively. Additionally, other compounds such as  $MgSO_4 \cdot 7H_2O$  (0.61g/L),  $MnSO_4 \cdot 4H_2O_2$  (2g/L),  $CaCl_2 \cdot 2H_2O$  (8.82g/L), and  $FeSO_4 \cdot 4H_2O$  (0.33g/L). The PH was set to 7.0 and then sterilized at 121 °C for 15 min by autoclaving. After sterilization, the medium left to cool and inoculated 2% of the selected bacteria isolate a 0.5 McFarland standard corresponds to  $1.5 \times 10^8$  CFU/ml. And cultured in a shaker incubator at 28 °C for 48 hrs at 120 revolutions per minute (rpm) (22).

**Extraction and purification of prodigiosin:** The prodigiosin was produced by using cell-free broth culture of *Serratiamarcescens* which in turn was acquired after an incubation period of 48 hrs. at 28 °C. The culture media was subject to the centrifuging process at 8000

rpm for 15 min. Continuously, the acquired supernatant was then discarded, while a particular amount of methanol (250 ml) was poured into the obtained cell; the mixture was systematically mixed for 3 hrs. at room temperature. The attained mixture (methanol and culture media) was, hereinafter, centrifuged at 8000 rpm. for 20 min where the supernatant was collected and filtered using specific filtering paper (0.2 µm, millipore filter). Consequently, the methanol filtrate was concentrated using a rotary evaporator at a temperature of 70 °C, while double the amount of chloroform was supplemented for the red pigment extraction. Both methanol and chloroform were mixed thoroughly using a reparatory funnel whereby the organic chloroform phase was separated and later dried at 45 °C. Finally, the obtained pigment was liquefied using a particular amount of methanol and deposited in a fridge using an opaque bottle for further use (7).

**Syntheses of zinc oxide nanoparticles:** ZnO nanoparticles were synthesized via the biological synthesis approach using zinc acetate  $[\text{Zn}(\text{CH}_3\text{CO}_2)_2]$  (15). In a typical procedure, 5 gm of zinc acetate was dissolved in deionized distilled water (DDW) using the sonication technique for 30 min (solution A). Concurrently, solution (B) was obtained by dissolving a certain amount of prodigiosin (10 mg/ml) using the aforementioned technique. Subsequently, both solutions (A and B) were mixed thoroughly using an ultra-sonication bath for 60 min; with a pH level of 7.0 and the temperature at 50 °C and later kept in a dark condition overnight. The resultant solution was then centrifuged and washed using deionized water several times. Hereinafter, the obtained weight residuals were dried at 60 °C and then kept in a dark condition for further use.

**Antibacterial test (in vitro):** The antibacterial activities of the biologically synthesized ZnO nanoparticles against Gram-negative *p. aeruginosa* were tested using the agar well diffusion technique in which the minimal inhibition concentration (MIC) of ZnO nanoparticles was estimated (23). Herein, Müller Hinton agar sterilized medium (25 ml) was added into the sterilized Petri dishes and allowed to solidify at laboratory conditions overnight. The grown test species were extended on the agar medium through the sterile cotton swab technique. Consequently,

variety of ZnO concentrations (5,10, 20, 40, 80, 160, and 320)  $\mu\text{g/ml}$  were poured into the pre-made wells. The attained plates were then inoculated for 24 hrs. at a temperature of 37 °C. Hereinafter, the zone of inhibitions was measured around the pre-made wells (24).

## RESULTS AND DISCUSSION

**Production of prodigiosin pigment:** The identification of the collected bacterial isolates for the production of prodigiosin was accomplished through a biological test so-called Vitek-2 compact system where the regarded outcomes are illustrated in Figure 1. The prodigiosin production was started after the incubation period (12 hrs.). Herein, the prodigiosin concentration (at the end of the exponential phase) was found to be 0.29 g/L at 48 hrs. of incubation and 0.4145 g/L (during the stationary phase) at 35 hrs. The alteration of the medium to red color noticed could be attributed to the prodigiosin production which was accumulated primarily throughout the stationary phase (25).

**Characterization of prodigiosin pigment:** The absorbance characteristics of the extracted prodigiosin using *S. marcescens* was achieved through UV-Vis spectrophotometer (Shimadzu, Japan) with a range of 400-600 nm (Figure 2). In particular, the maximum absorption was noticed at around 525 nm which is in good agreement with previous studies (25).

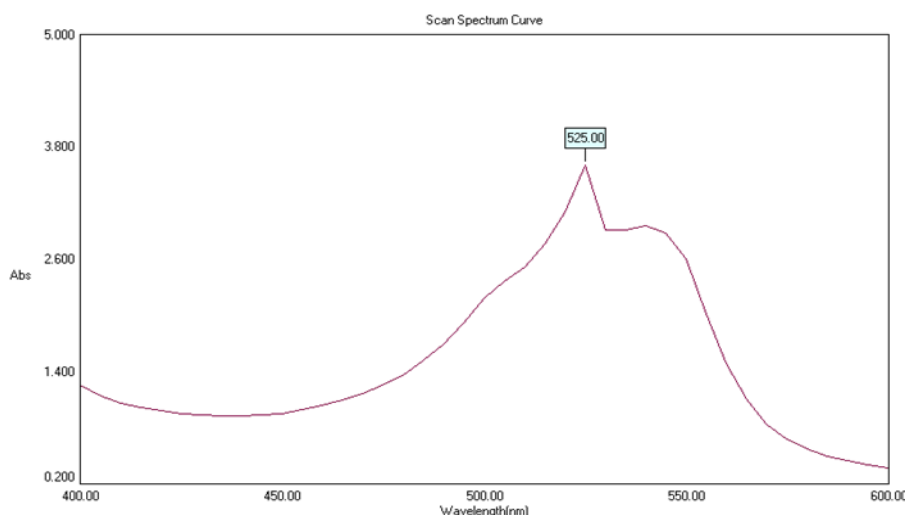


**Figure 2.** Absorption spectra of the purified pigment, extracted from *Serratia* spp

**Ultra-violet visible light (UV-Vis) analysis:** The optical properties of the biosynthesized ZnO NPs was examined using UV-Vis spectroscopy technique. As demonstrated in Figure 3, the attained ZnO NPs exhibited a

pronounced UV absorption at around 287 nm. The stated absorption could be mainly attributed to the biosynthesized ZnO's direct band emission (12, 18).

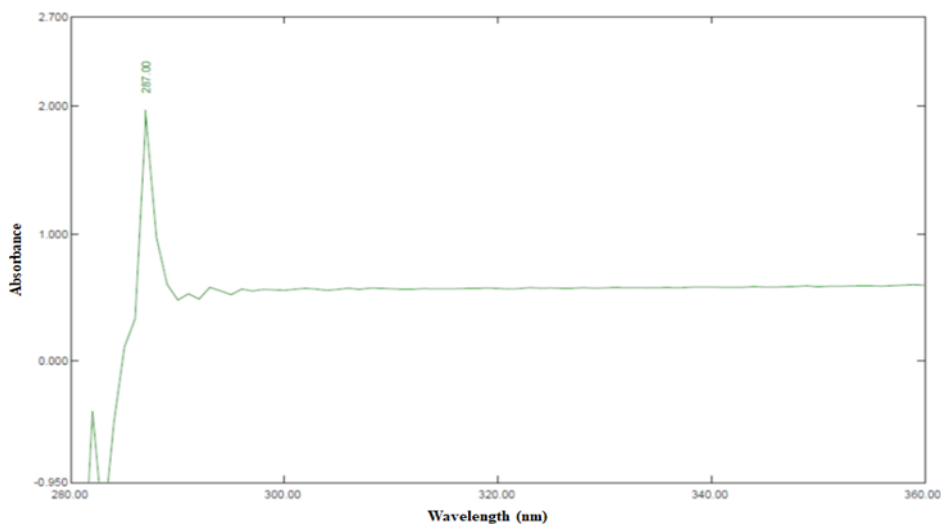


**Figure 3. UV-Vis spectrum of the biosynthesized ZnO**

**Atomic force microscopy (AFM) analysis:**  
The AFM was introduced to investigate the ZnO nanoparticles' surface features using a 2D and 3D imaging approach (Figure 4).

Specifically, the AFM outcomes revealed that the ZnO nanoparticles exhibit a spherical shape with an average diameter size of 45.02 nm.

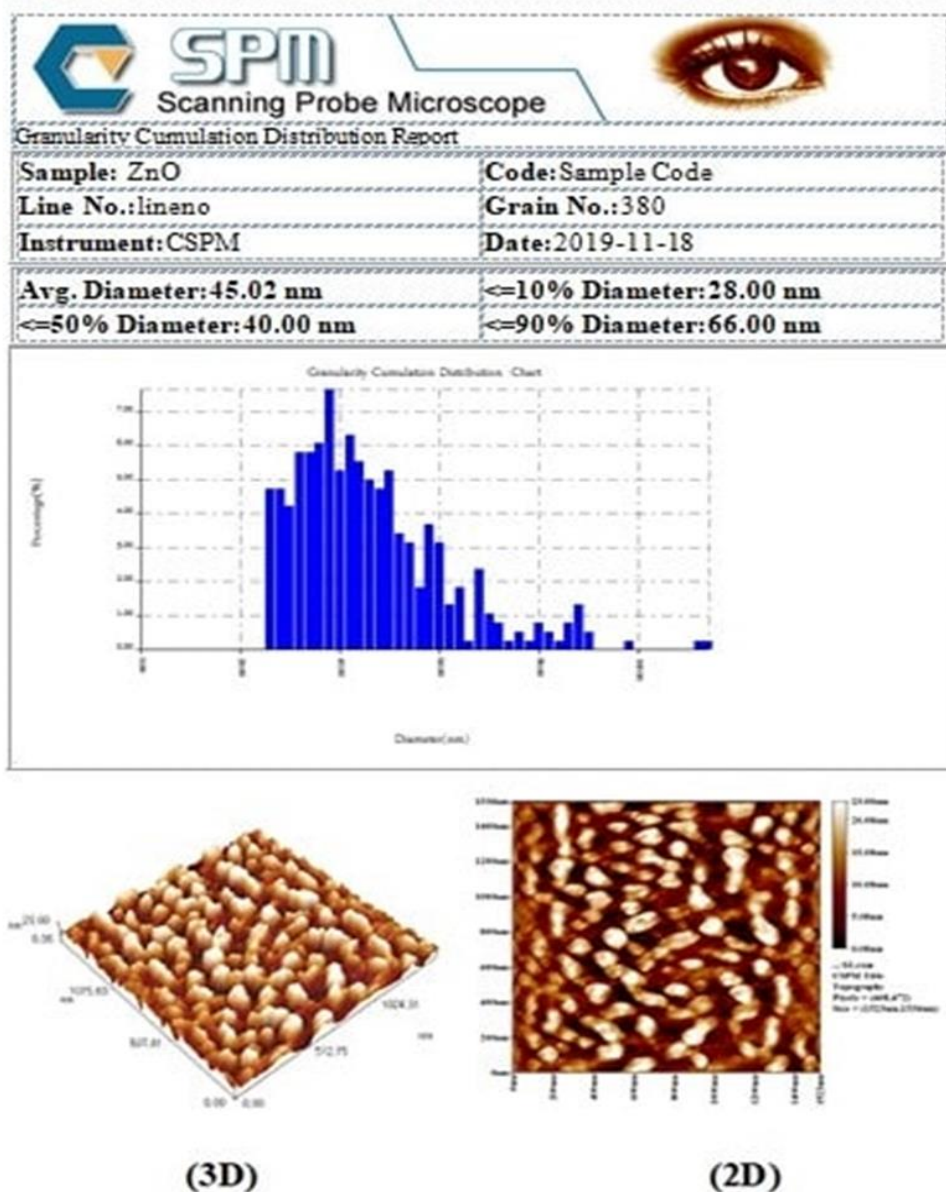


**Figure 4. Atomic Force Microscopy of the bio-synthesized ZnO**

**X-ray diffraction (XRD) analysis:** The XRD patterns obtained from the bio-synthesized ZnO nanoparticles is elucidated in Figure 5. Continuously, three pronounced peaks were observed between  $2\theta = 30$  to 40 degrees (JCPDS No. 89-1397) which can be indexed to the occurrence of metal oxide ZnO nanoparticles hexagonal phase wurtzite structure (26). In the meanwhile, the crystalline particles were calculated using the well-known Debye-Scherrer equation:

$$D = \left[ \frac{K\lambda}{\beta \cos\theta} \right] \text{Å}$$

Herein, the crystallite size is represented by the symbol ( $D$ ), while  $K$  denotes the shape factor which is a constant (0.9) and  $\lambda$  is the x-ray wavelength (1.5406 Å). The Bragg angle and corrected line broadening of the nanoparticles are represented by the symbols  $\theta$  and  $\beta$ , respectively.

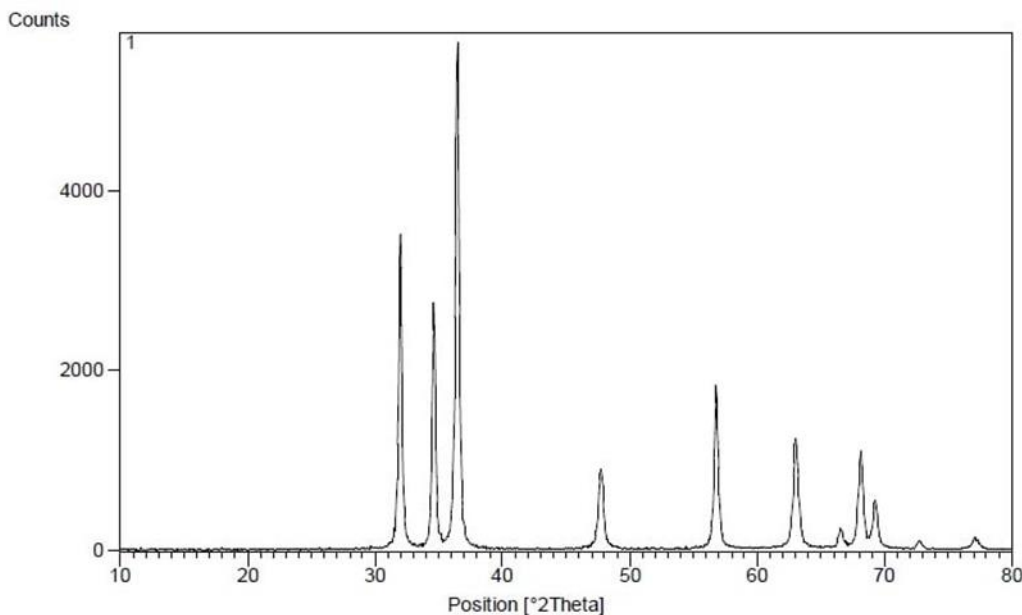


**Figure 5. XRD patterns of the bio-synthesized ZnO nanoparticles**

**Fourier transforms infrared (FTIR) spectroscopy analysis:** The FT-IR results for the bio-synthesized ZnO nanoparticles are demonstrated in Figure 5. Generally, absorption peaks series ranging between 400 to 4000  $\text{cm}^{-1}$  could be noticed which are corresponded to the hydroxyl and carboxylate in materials. Particularly, a broadband around 3120.61  $\text{cm}^{-1}$  is attributed to the

stretching mode of the C-Haromatics group. In the meanwhile, other peaks located within the 1560.30  $\text{cm}^{-1}$  are mainly caused by the stretching vibration of N-O (Nitrocompounds). Furthermore, peak perceived at 1446.51  $\text{cm}^{-1}$  is attributed to the stretching mode of C-C (in-ring) aromatics, and 694.33  $\text{cm}^{-1}$  are metal oxygen attributed to symmetrical as well as asymmetrical zinc carboxylate stretching (27).

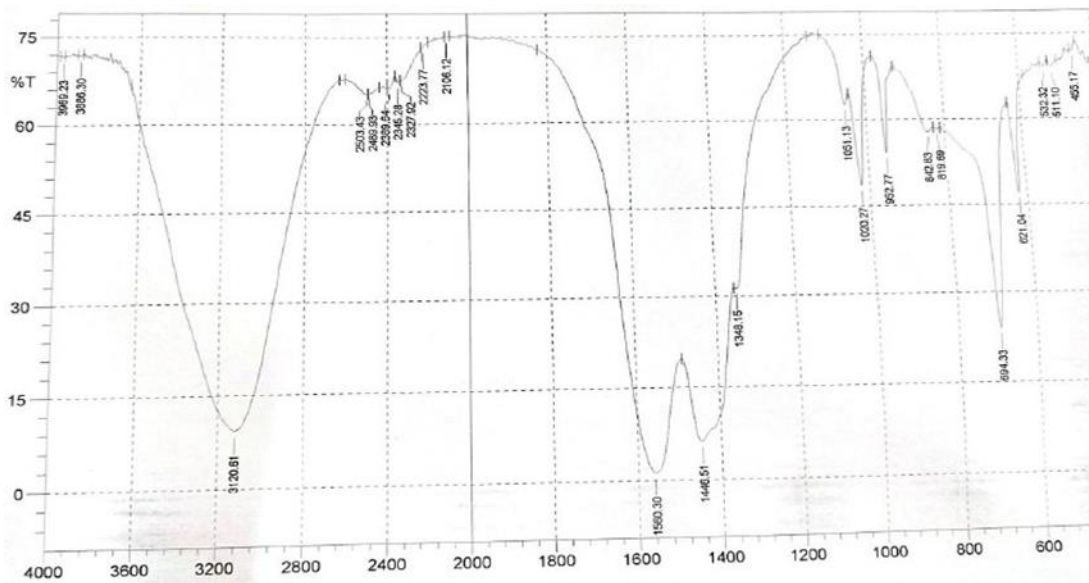


Figure 5. FTIR spectrum of the biosynthesized ZnO

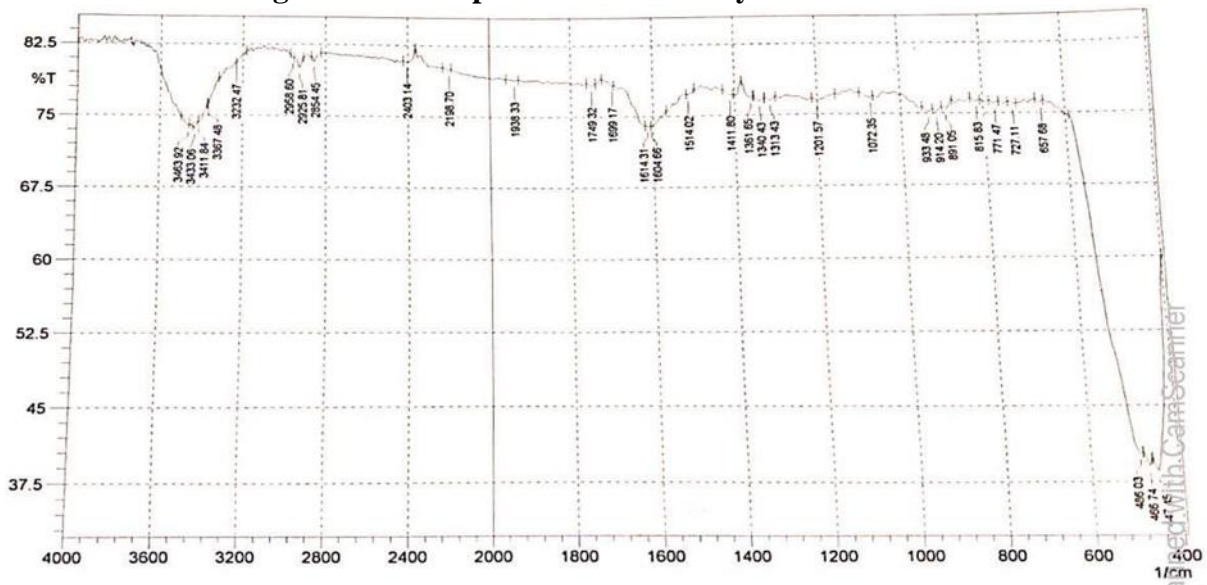


Figure 6. FTIR spectrum of the biosynthesized nano

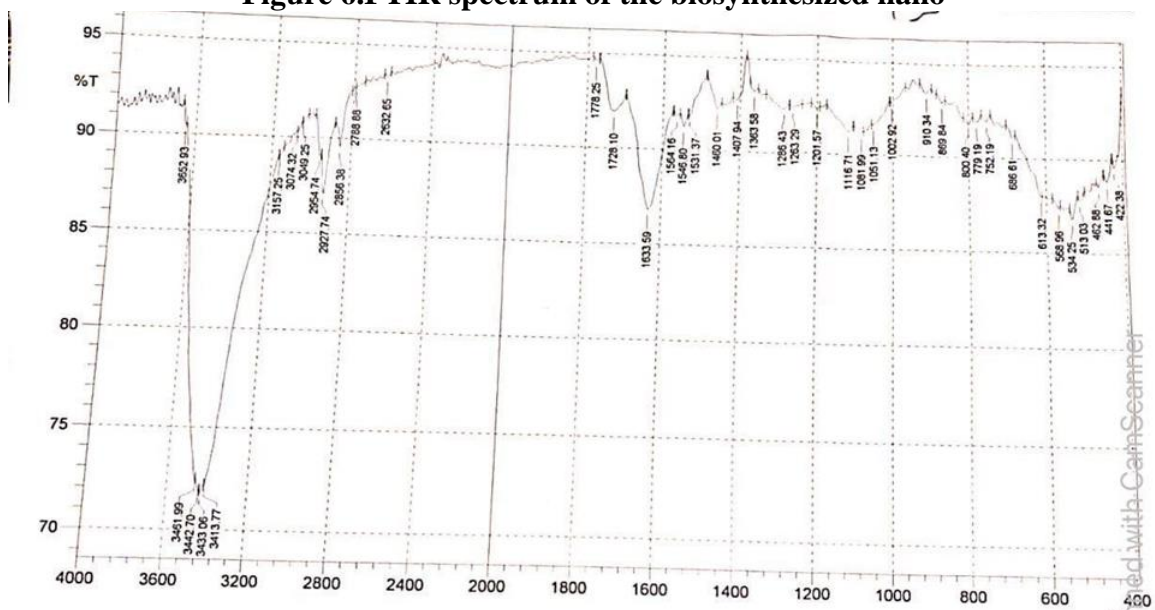
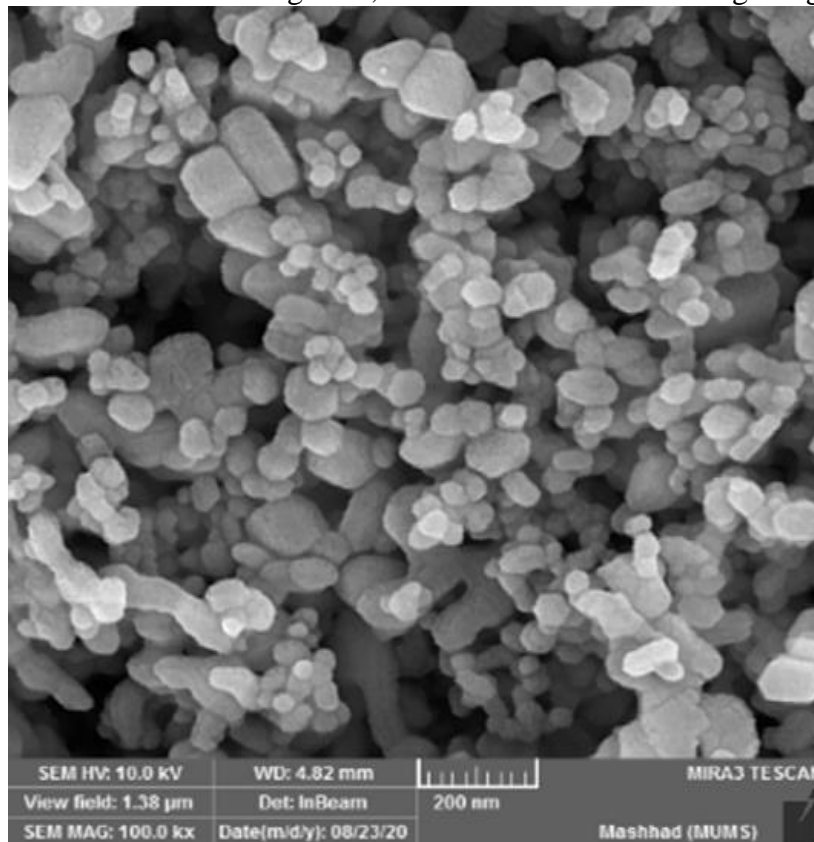


Figure 7. FTIR spectrum of the biosynthesized prodigiosin pigment

**Field emission scanning electron microscopy (FE-SEM) analysis:** The morphological properties of the bio-synthesized ZnO NPs were examined using the FE-SEM technique. As illustrated in Figure 6,

the prepared ZnO NPs sample exhibited spherical particles as well as plate-like structures. It is worth mentioning that the average nanoparticles diameter was found to be around 40 nm using ImageJ software.



**Figure 8.**FE-SEM image of the bio-synthesized ZnO nanoparticles

**Antibacterial susceptibility test:** The antibacterial activity of the bio-synthesized ZnO nanoparticles at different concentrations (5,10, 20, 40, 80, 160, and 320)  $\mu\text{g/ml}$  is depicted in Figure 7 and Table 1. It is clear to be noticed that the ZnO NPs antibacterial activity is directly dependent on the utilized concentrations. Furthermore, Table 1 reveals that the concentration as low as 5  $\mu\text{g/ml}$  of ZnO did not show any zone of inhibition, while an inhibition zone of 29mm was acquired at a ZnO concentration of 320 $\mu\text{g/ml}$ . The range in the inhibition zone, demonstrated in Table 1, could be attributed to different ZnO interaction mechanism with the microorganism utilized as well as the bacteria susceptibility. The ZnO NPs toxicity on any bacteria is

mainly due to the reactive oxygen species (ROS) generation. Specifically, the ROS toxicity to the cell's wall is attributed to the cellular constituent damage like proteins, lipids, and DNA. The generation of ROS is widely considered as the major factor of antibacterial activity associated with the ZnO phototoxicity(28, 29). This in turn leads to oxidation which in turn kills/inhibits the microorganisms. Using the serial dilution method, the MIC was evaluated with a range of 5-320 $\mu\text{g/mL}$  as pre-described CLSI (30, 31).The antibacterial activity of ZnO NPs is of great importance because of the pathogenetic bacteria's ability in joining the ecosystem food chain(32).



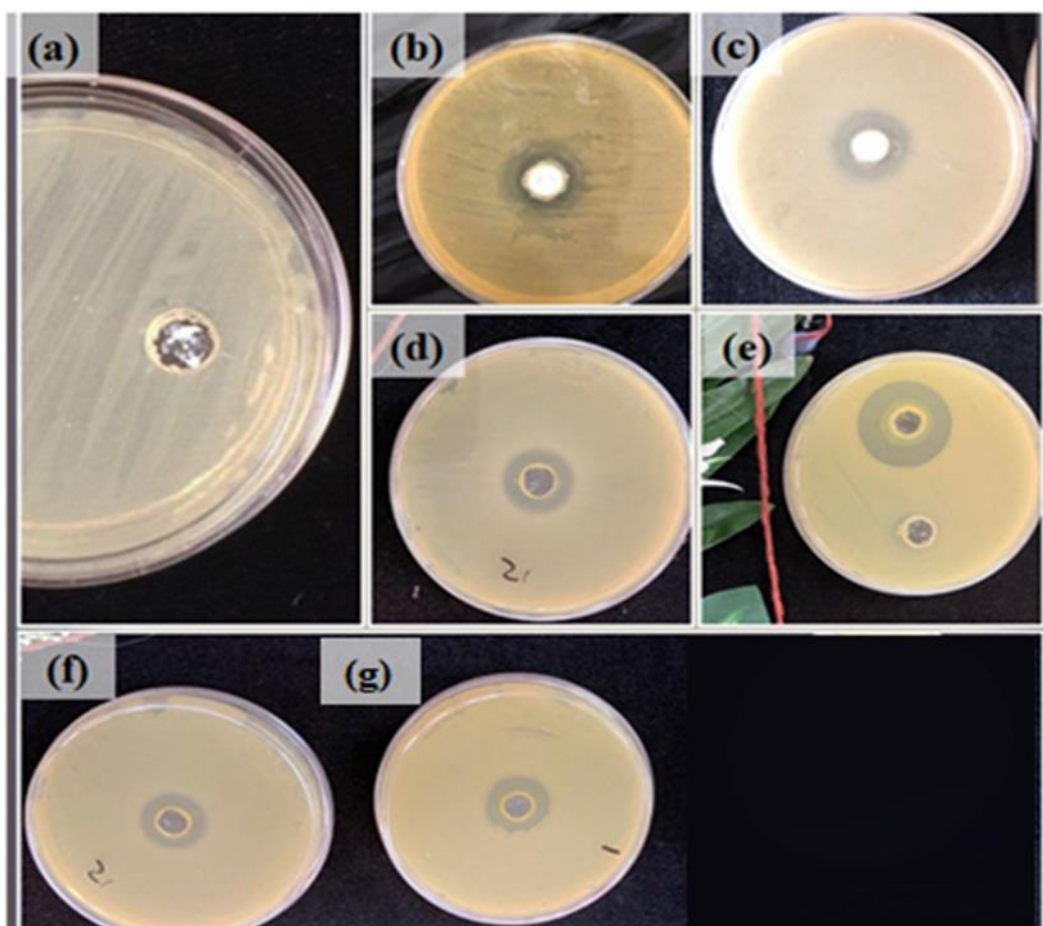


Figure 9. Antibacterial activity of the bio-synthesized ZnO nanoparticles against *pseudomonas aeruginosa* at concentration of (a) 5, (b) 10, (c) 20 (d) 40, (f) 80, (g) 160 and (e) 320µg/ml

Table 1. Inhibition zone of ZnO nanoparticles

ZnO concentration (µg/mL)	Inhibition zone (mm)
5	Nil
10	7
20	15
40	19
80	21
160	25
320	29

## CONCLUSION

In this study, the biosynthesis of ZnO nanoparticles using prodigiosin as a reducing agent was demonstrated successfully. Additionally, the attained ZnO NPs were characterized using UV-Vis, AFM, XRD, FT-IR, and FE-SEM. Techniques. In particular, The XRD patterns showed the successful ZnO NPs phase formation, while the FE-SEM demonstrated that the prepared ZnO NPsexhibited spherical particles as well as plate-like structures with an average diameter size ranging between 30-50 nm. While the AFM revealed an average diameter of 45.02 nm. In the antibacterial activity test, it was

found that the bio-synthesized has a strong antibacterial activity against the introduced bacteria. The maximum inhibition zone was found to be 29 mm at a concentration of 320 µg/mL.

## REFERENCES

1. A.C. Gales, P.L. Torres, D.S. Vilarinho, R.S. Melo, C.F. Silva, R.F.Cereda and Carbapenem.2004.Resistant *Pseudomonas aeruginosa* outbreak in an intensive care unit of a teaching hospital, *Brazilian Journal of Infectious Diseases*, 8: 267-271
2. A.A. Ramos, A. Azqueta, C. Pereira-Wilson and A.R. Collins.2010. Polyphenolic compounds from *Salvia* species protect

cellular DNA from oxidation and stimulate DNA repair in cultured human cells, *Journal of agricultural and food chemistry*, 58 :7465-7471

3. B. Forbes, D. Sahm, and A. Weissfeld.2002. Laboratory methods for detection of antibacterial resistance, *Bailey & Scott's Diagnostic Microbiology*, 230-231

4. D. Ferguson. 2008. A study of clinical strains of *Pseudomonas aeruginosa* and the investigation of antibiotic resistance mechanisms in the multidrug resistant strain PA13, in, *Dublin City University*

5. E.A. Menezes, L.A. Silveira, F.A. Cunha, M.d.S. Cavalcante, A.B. Teixeira, I.R.N. Oliveira and M.N.C. Salviano.2003. Perfil de resistência aos antimicrobianos de *Pseudomonas* isoladas no Hospital Geral de Fortaleza, *Rev. bras. anal. clin.*, 177-180

6. E.Bergogne-Berezin.2004. *Pseudomonas* and miscellaneous gram-negative bacilli, *Infectious diseases*, 2 : 2203-2226

7. E. Rokhsat, O. Akhavan.2016. Improving the photocatalytic activity of graphene oxide/ZnO nanorod films by UV irradiation, *Applied Surface Science*, 371 : 590-595

8. E.M. Tretter, J. M. Berger. 2012. Mechanisms for defining supercoiling set point of DNA gyrase orthologs II. The shape of the gyra subunit C-terminal domain (CTD) is not a sole determinant for controlling supercoiling efficiency, *Journal of Biological Chemistry*, 287 : 18645-18654

9. E.Y. Salih, M.F.M. Sabri, S.T. Tan, K. Sulaiman, M.Z. Hussein, S.M. Said and C.C. Yap.2019. Preparation and characterization of ZnO/ZnAl<sub>2</sub>O<sub>4</sub>-mixed metal oxides for dye-sensitized photodetector using Zn/Al-layered double hydroxide as precursor, *Journal of Nanoparticle Research*, 21 :55

10. E.Y. Salih, M.F.M. Sabri, M.H. Eisa, K. Sulaiman, A. Ramizy, M.Z. Hussein and S.M. Said, Mesoporous ZnO/ZnAl<sub>2</sub>O<sub>4</sub> mixed metal oxide-based Zn/Al layered double hydroxide as an effective anode material for visible light photodetector, *Materials Science in Semiconductor Processing*, 121 105370

11. E.Y. Salih, M.F.M. Sabri, K. Sulaiman, M.Z. Hussein, S.M. Said, R. Usop, M.F.M. Salleh and M.B.A. Bashir.2018. Thermal, structural, textural and optical properties of ZnO/ZnAl<sub>2</sub>O<sub>4</sub> mixed metal oxide-based Zn/Al

layered double hydroxide, *Materials Research Express*, 5 : 116202

12. E.Y. Salih, M.F.M. Sabri, M.Z. Hussein, K. Sulaiman, S.M. Said, B. Saifullah and M.B.A. Bashir. 2018. Structural, optical and electrical properties of ZnO/ZnAl<sub>2</sub>O<sub>4</sub> nanocomposites prepared via thermal reduction approach, *Journal of Materials Science*, 53 : 581-590

13. F. Malega, I. Indrayana, E. Suharyadi. 2018. Synthesis and characterization of the microstructure and functional group bond of Fe<sub>3</sub>O<sub>4</sub> nanoparticles from natural iron sand in Tobelo North Halmahera, *Jurnal Ilmiah Pendidikan Fisika Al-Biruni*, 7 :13-22

14. G. Xiong, U. Pal, J. Serrano, K. Ucer and R. Williams. 2006. Photoluminescence and FTIR study of ZnO nanoparticles: the impurity and defect perspective, *physica status solidi c*, 3 :3577-3581

15. I. Machado, J. Graça, H. Lopes, S. Lopes and M.O. Pereira.2013. Antimicrobial pressure of ciprofloxacin and gentamicin on biofilm development by an endoscope-isolated *Pseudomonas aeruginosa*, *ISRN biotechnology*

16. Jayarambabu, N., Kumari, B. S., Rao, K. V., and Prabhu Y. T. 2014. Germination and growth characteristics of mungbean seeds (*Vignaradiata* L.) affected by synthesized zinc oxide nanoparticles. *International Journal of Current Engineering and Technology*, 4(5), 2347-5161

17. K. Shim, M. Abdellatif, E. Choi, D. Kim.2017. Nanostructured ZnO films on stainless steel are highly safe and effective for antimicrobial applications, *Applied microbiology and biotechnology*, 101: 2801-2809

18. L. Zhang, Y. Jiang, Y. Ding, N. Daskalakis, L. Jeuken, M. Povey, A.J. O'Neill and D.W. York.2010. Mechanistic investigation into antibacterial behaviour of suspensions of ZnO nanoparticles against *E. coli*, *Journal of Nanoparticle Research*, 12 :1625-1636

19. M. Abd Al-Mayali, E.D. Salman.2020. Bacteriological and Molecular Study of Fluoroquinolones Resistance in *Pseudomonas aeruginosa* Isolated From Different Clinical Sources, *Iraqi Journal of Science*, 2204-2214

20. N. Hussein.2019. Detection of the antibacterial activity of AgNPs biosynthesized by *Pseudomonas aeruginosa*, Iraqi Journal of Agricultural Science, 50 : 617-625
21. N.K. Abbas, A.A. Al-Attraqchi.2020. Antimicrobial Activities of Green Biosynthesized Iron Oxide Nanoparticles Using *F. Carica* Fruit Extract, Indian Journal of Forensic Medicine & Toxicology, 14 : 2181-2187
22. N. Al-Gbouri, A. Hamzah.2018. Evaluation of phyllanthus emblica extract as antibacterial and antibiofilm against biofilm formation bacteria, Iraqi Journal of Agricultural Sciences, 49:142-151
23. P.K. Stoimenov, R.L. Klinger, G.L. Marchin, K.J. Klabunde.2002. Metal oxide nanoparticles as bactericidal agents, Langmuir, 18 : 6679-6686
24. P. Edwards, and W. H. Ewing. 1972. Identification of Enterobacteriaceae, Burgess Publishing Co., J. CLIN. MICROBIOL. neonatal meningitis. J. Neurosurg, 52 : 547-552
25. R. Saravanan, V. Gupta, V. Narayanan, A. Stephen.2014. Visible light degradation of textile effluent using novel catalyst ZnO/ $\gamma$ -Mn<sub>2</sub>O<sub>3</sub>, Journal of the Taiwan Institute of Chemical Engineers, 45 :1910-1917
26. R. Salomoni, P. Léo, A. Montemor, B. Rinaldi and M. Rodrigues.2017. Antibacterial effect of silver nanoparticles in *Pseudomonas aeruginosa*, Nanotechnology, science and applications, 10 : 115.
27. R.P. Williams, C.L. Gott, J.A. Green.1961.STUDIES ON PIGMENTATION OF *SERRATIA MARCESCENS* V.: Accumulation of Pigment Fractions with Respect to Length of Incubation Time1, Journal of bacteriology, 81 :376
28. R. Facklam.1973. Comparison of several laboratory media for presumptive identification of enterococci and group D streptococci, Applied microbiology, 26 : 138-145
29. S. Azizi, M. Ahmad, M. Mahdavi, S. Abdolmohammadi.2013. Preparation, characterization, and antimicrobial activities of ZnO nanoparticles/cellulose nanocrystal nanocomposites, BioResources, 8 : 1841-1851
30. S.H. Korji.2012. Inhibition of Nitrate Reductase Production from Gram-Negative Bacteria Using *Zizyphus Spina-Christi* Extract and Comparing with some Antibiotics, Iraqi Journal of Agricultural Science, 43 : 144-150
31. V. Kononenko, N. Repar, N. Marušič, B. Drašler, T. Romih and S. Hočevar, Drobne.2017. Comparative in vitro genotoxicity study of ZnO nanoparticles, ZnO macroparticles and ZnCl<sub>2</sub> to MDCK kidney cells: Size matters, Toxicology in Vitro, 40 : 256-263
32. W.-C. Chen, W.-J. Yu, C.-C. Chang, J.-S. Chang, S.-H. Huang, C.-H. Chang, S.-Y. Chen, C.-C. Chien, C.-L. Yao and W.-M. Chen.2013. Enhancing production of prodigiosin from *Serratia marcescens* C3 by statistical experimental design and porous carrier addition strategy, Biochemical engineering journal, 78 : 93-100.